

Obstacles to two-line Josephson traveling wave parametric amplifier

Victor K. Kornev, Alena N. Nikolaeva, Nikolay V. Kolotinskiy

Abstract—Obstacles to the two-line Josephson traveling wave parametric amplifier (JTWPA) designs, aimed at increasing the allowed pump wave energy and, hence, the gain growth through the combination of linear and nonlinear lines as pump and signal lines is discussed. This analysis takes into account both the mutual coupling and the discreteness of the artificial waveguide lines. Significant restrictions arise from the cyclical transfer of the traveling wave's energy from one line to the other one with phase step by π every beat cycle. Moreover, the other restrictions result from the phase mismatch between the pump, signal and idler waves due to both the coupling and the discreteness of the artificial lines.

Index Terms—Traveling wave amplifiers, Josephson devices, Josephson amplifiers, parametric devices, Josephson traveling-wave parametric amplifier (JTWPA).

I. INTRODUCTION

THE parametric amplification mechanism enables extremely high-sensitive amplifiers capable of showing noise temperature T_N lower than the ambient temperature. A traveling wave design concept of the amplifiers allows overcoming the gain-bandwidth trade-off which is attributable to the cavity-based parametric amplifiers. Superconductive Josephson Traveling Wave Parametric Amplifiers (JTWPAs) are capable of working at low and very low temperatures and capable of approaching quantum limit sensitivity. Therefore, the amplifiers are considered promising readout devices in the fields of precision quantum measurements, quantum communications and quantum computing (e.g., see [1]–[3], and review [4]). As shown schematically in Fig. 1, these amplifiers are based on the use of artificial discrete waveguide lines of LC-cells each composed of a linear capacitor C and nonlinear L -element. The latter is usually either a single Josephson junction or a Superconducting Quantum Interference Device (SQUID) containing one, two or several Josephson junctions. In the general case, the L -element can combine both the geometric inductance and the strongly nonlinear kinetic inductance of the Josephson junctions

$$L_J = L_{J0} / \cos(\varphi) \quad (1)$$

which is attributable to the superconducting current component of the used junctions:

$$I_s = I_c \sin(\varphi), \quad (2)$$

Manuscript received July 25, 2024; revised November 05, 2024 and January 02, 2025.

This research was funded by Russian Science Foundation (RSCF) grant no. 19-72-10016-P.

Victor K. Kornev, Alena N. Nikolaeva and Nikolay V. Kolotinskiy are with Department of Physics, Lomonosov Moscow State University, 119991, Moscow, Russia. Any correspondence should be addressed to Nikolay V. Kolotinskiy (kolotinskiy@physics.msu.ru).

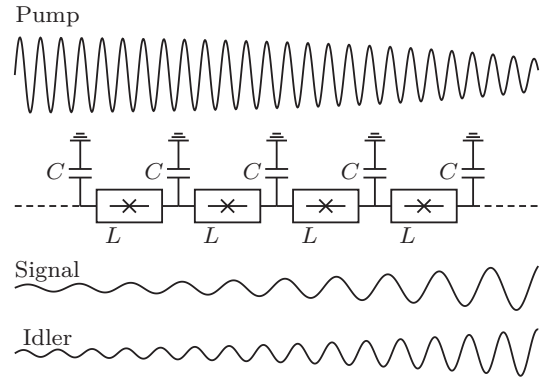


Fig. 1. Illustration of a TWPA composed of a chain of Josephson-junction cells with propagating pump, signal, and idler waves.

where I_c and φ are the junction critical current and phase, respectively; $L_{J0} = \Phi_0 / (2\pi I_c)$ is the characteristic value of the junction inductance, and $\Phi_0 = h / (2e)$ is the magnetic flux quantum.

Nonlinear interaction between the pump and signal waves applied initially to the line input originates an idler wave. Subsequent nonlinear interaction of three waves propagating along the line yields in the energy transfer from the high-power pump wave to both the signal and idler waves. The relation between frequencies ω_p , ω_s , ω_i of the pump, signal and idler waves, respectively, depends on the exploited mixing mode. Quadratic nonlinearity allows the use of a three-wave-mixing mode (3WM), when the frequencies obey the relation

$$\omega_s + \omega_i = \omega_p \quad (3)$$

and the wave vectors obey the relation

$$k_p = k_s + k_i \quad (4)$$

needed to achieve the required phase matching of the waves in the 3WM mode.

Cubic (Kerr) nonlinearity allows the use of four-wave-mixing mode (4WM) when the frequencies obey the following relation:

$$\omega_s + \omega_i = 2\omega_p \quad (5)$$

and the wave vectors obey the relation

$$2k_p = k_s + k_i \quad (6)$$

needed to achieve the required phase matching of the waves in the 4WM mode.

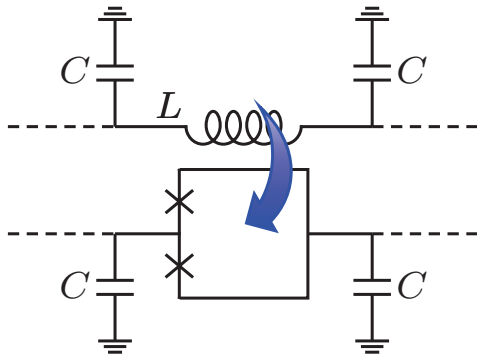


Fig. 2. A fragment of the flux driven JTWPA [11] composed of two artificial waveguide lines, which are (1) linear LC line and (2) nonlinear Josephson line containing dc SQUIDs as nonlinear L -elements. In the design, the pump wave current, flowing in the linear inductances L of the first line, applies magnetic flux to the dc SQUID cells of the second (signal) line. This provides modulation of the signal line cells inductances in a traveling wave pattern.

The achievable gain depends on several factors [5]–[8], among which is the pump wave depletion with the energy transfer to the signal and idle waves, as well as to the higher pump harmonics and undesired intermodulation components [9], [10]. The depletion cannot be balanced with the starting power of the pump wave since the pump wave amplitude is restrained by the critical-current value of the Josephson junctions used.

To overcome the gain limitation, a flux-driven JTWPA has been proposed [11] although is not still realized. The amplifier is composed of two artificial lines, namely of a nonlinear Josephson line and a linear LC line meant for propagation of a high-power pump wave. The pump wave current, flowing in the inductances L of the linear line, applies magnetic flux to the dc SQUID cells of the second (signal) line as shown in Fig. 2. This results in modulation of the cell inductances along the line in a traveling wave pattern [11], [12] as follows:

$$L = L_0 (1 + m \cdot \cos(\omega_p t - k_p x)), \quad (7)$$

where m is modulation depth, and L_0 is the reference SQUID-cell inductance controlled by the dc magnetic flux which is additionally applied. Such a modulation relation allows realizing the three-wave-mixing mode (3), when the required phase-matching condition (4) is fulfilled as well.

The flux driven JTWPA can be considered as a particular case of a more general design concept of the two-line JTWPAs, composed of a nonlinear Josephson waveguide line and a linear artificial LC waveguide line meant for propagation of a high-power pump wave. The linear line is supposed to be used as a pump wave energy source for the nonlinear Josephson line in order to balance (through coupling elements) the pump wave power depletion and hence to support the fixed pump wave amplitude in this waveguide line. However, as a matter of fact, this design concept implies realizing a completely nonreciprocal coupling between the two waveguide lines. Unfortunately, this cannot be obtained at least with using the linear electromagnetic linkage. Therefore, one should take

into account the inevitable mutual coupling between the two waveguide lines.

For example, practically all the real designs meant to answer to the schematic shown in Fig. 2 for the flux-driven JTWPA give concurrently two effects. Namely, the pump wave current in the first (linear) line concurrently (i) applies magnetic flux to the dc SQUID cells of the second line and (ii) induces an electromotive difference along the cell as the nonlinear inductance of the second (signal) line. The latter results from the inevitable spatial design asymmetry. In fact, when the cell inductance L of the first line is coupled magnetically mainly with the nearest loop side of the SQUID cell, the pump wave current $I_p = I_0 e^{-i\omega_p t}$ induces in the loop part the electromotive difference $V_{em} = i\omega_p M I_p$, where M is the mutual inductance between this loop part and inductance L . This electromotive difference produces both the circular ac current and ac voltage drop across the SQUID cell (between opposite points of the cell):

$$U = \frac{1}{2} M \frac{dI_p}{dt} = i\omega_p \frac{M}{2} I_p. \quad (8)$$

This expression evidences the mutual coupling between these waveguide lines through the effective mutual inductance $M/2$ between cells of the lines.

In common with two coupled oscillatory circuits, such coupling between the waveguide lines radically alters the whole wave process in the system. Given the increased interest in possible JTWPA designs based on two artificial lines such as the proposed flux-driven JTWPA, it is completely reasonable to consider the wave processes occurring in the coupled lines in terms applicable to the JTWPA designs.

In this paper, we analyze the obstacles to the two-line JTWPA designs taking into account both the mutual coupling and discreteness of the artificial lines used.

II. CONSIDERATION OF TWO COUPLED LINEAR WAVEGUIDES

A comprehensive study of the traveling wave parametric amplifiers based on the use of nonlinear waveguide lines must be conducted using numerical simulations or by solving a complex set of the coupled-mode-equations (e.g. see [5]). The presence of nonlinear reactive elements, which are needed for the parametric amplification process, complicates the device dynamics through generation of both the wanted and unwanted spectral components. However, the device functioning is inherently based on the wave propagation process, which can be radically changed by coupling between the waveguide lines. Basically, this change can be studied through considering two coupled linear waveguide lines as done below.

Fig. 3 shows equivalent circuits of two coupled linear waveguide lines with capacitive (a) and inductive (b) couplings realized through either linking capacitance C_0 or the mutual inductance M , respectively. In the continuum approximation, the telegraph equations for the first system can be written as follows:

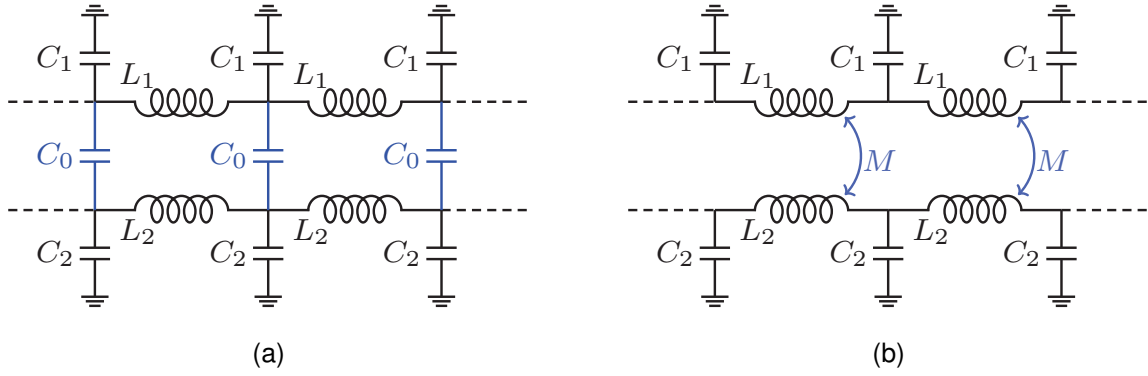


Fig. 3. Equivalent circuits of two coupled linear waveguide lines with capacitive (a) and inductive (b) couplings realized through either the linking capacitance C_0 or the mutual inductance M , respectively.

$$\frac{\partial U_1}{\partial x} = -L_1 \frac{\partial I_1}{\partial t}, \quad \frac{\partial I_1}{\partial x} = -C_1 \frac{\partial U_1}{\partial t} - C_0 \frac{\partial(U_1 - U_2)}{\partial t}, \quad (9)$$

$$\frac{\partial U_2}{\partial x} = -L_2 \frac{\partial I_2}{\partial t}, \quad \frac{\partial I_2}{\partial x} = -C_2 \frac{\partial U_2}{\partial t} - C_0 \frac{\partial(U_2 - U_1)}{\partial t}, \quad (10)$$

where $U_{1,2}$ and $I_{1,2}$ are the voltage and the current in the first and second lines, respectively. These equations yield in the following set of two coupled wave equations:

$$v_{01}^2 \frac{\partial^2 U_1}{\partial x^2} = \frac{\partial^2 U_1}{\partial t^2} - \alpha_1 \frac{\partial^2 U_2}{\partial t^2}, \quad (11)$$

$$v_{02}^2 \frac{\partial^2 U_2}{\partial x^2} = \frac{\partial^2 U_2}{\partial t^2} - \alpha_2 \frac{\partial^2 U_1}{\partial t^2}, \quad (12)$$

where $v_{01}^2 = (L_1 C_1)^{-1}$, $v_{02}^2 = (L_2 C_2)^{-1}$ are the squared phase velocities in the separate (uncoupled) lines, $\alpha_1 = C_0/(C_1 + C_0) \approx C_0/C_1$, $\alpha_2 = C_0/(C_2 + C_0) \approx C_0/C_2$ are the capacitive coupling factors of the lines. In case of inductive coupling, telegraph equations are as follows:

$$\frac{\partial U_1}{\partial x} = -L_1 \frac{\partial I_1}{\partial t} - M \frac{\partial I_2}{\partial t}, \quad \frac{\partial I_1}{\partial x} = -C_1 \frac{\partial U_1}{\partial t}, \quad (13)$$

$$\frac{\partial U_2}{\partial x} = -L_2 \frac{\partial I_2}{\partial t} - M \frac{\partial I_1}{\partial t}, \quad \frac{\partial I_2}{\partial x} = -C_2 \frac{\partial U_2}{\partial t}, \quad (14)$$

and yield in the similar set of two coupled wave equations:

$$v_{01}^2 \frac{\partial^2 I_1}{\partial x^2} = \frac{\partial^2 I_1}{\partial t^2} - \eta_1 \frac{\partial^2 I_2}{\partial t^2}, \quad (15)$$

$$v_{02}^2 \frac{\partial^2 I_2}{\partial x^2} = \frac{\partial^2 I_2}{\partial t^2} - \eta_2 \frac{\partial^2 I_1}{\partial t^2}, \quad (16)$$

where $v_{01}^2 = (L_1 C_1)^{-1}$, $v_{02}^2 = (L_2 C_2)^{-1}$ are the squared phase velocities in the separate (uncoupled) lines, $\eta_1 = M/L_1$, $\eta_2 = M/L_2$ are the inductive coupling factors of the lines.

Due to the complete similarity between the wave equations sets (11), (12) and (15), (16), one can consider the only first equations set and look for its solution as

$$U_1 = A \cos(\omega t - kx), \quad U_2 = B \cos(\omega t - kx). \quad (17)$$

In this case, (11) and (12) gives the following system of two linear equations for the wave amplitudes:

$$(k^2 v_{01}^2 - \omega^2) A + \alpha_1 \omega^2 B = 0, \quad (18)$$

$$\alpha_2 \omega^2 A + (k^2 v_{02}^2 - \omega^2) B = 0. \quad (19)$$

Equating determinant of the equations set to zero, one comes to the following master equation

$$(k^2 v_{01}^2 - \omega^2) (k^2 v_{02}^2 - \omega^2) - \alpha_1 \alpha_2 \omega^4 = 0. \quad (20)$$

The master equation solution gives two values for the squared wave vector k^2 and hence two values for the squared phase velocity $v^2 = \omega^2/k^2$.

A. Identical waveguide lines

In the case of identical lines, when $v_{01}^2 = v_{02}^2 = v_0^2$ and $\alpha_1 = \alpha_2 = \alpha$, the master equation solution is as follows:

$$k^2 = \frac{\omega^2}{v_0^2} (1 \pm \alpha), \quad (21)$$

$$v^2 = \frac{v_0^2}{(1 \pm \alpha)} \approx v_0^2 (1 \mp \alpha), \quad (22)$$

$$k_{1,2} = \frac{\omega}{v_0} \left(1 \pm \frac{\alpha}{2}\right) = k_0 \pm \Delta k, \quad (23)$$

$$v_{1,2} = \frac{v_0}{(1 \pm \frac{\alpha}{2})} \approx v_0 \left(1 \mp \frac{\alpha}{2}\right) = v_0 \mp \Delta v, \quad (24)$$

where $k_0 = \omega/v_0$, $\Delta k = (\alpha/2) k_0$, and $\Delta v = (\alpha/2) v_0$.

Thus, the wave process in both lines consists of two waves having different phase velocities. The amplitude ratio can be easily obtained from the equations set (18) and (19):

$$\chi_{1,2} \equiv \left. \frac{B}{A} \right|_{k_{1,2}} = \frac{\alpha \omega^2}{(k^2 v_0^2 - \omega^2)} = \frac{\alpha}{(1 \pm \alpha) - 1} = \pm 1. \quad (25)$$

And therefore, the wave process in the lines can be written as follows:

$$U_1 = A_1 \cos(\omega t - k_1 x) + A_2 \cos(\omega t - k_2 x), \quad (26)$$

$$U_2 = A_1 \cos(\omega t - k_1 x) - A_2 \cos(\omega t - k_2 x). \quad (27)$$

When rf signal source $U = A \cos(\omega t)$ is applied to input of the only one of these two lines, *e.g.* to the first line, it corresponds to the following simple boundary conditions:

$$A_1 + A_2 = A, \quad A_1 - A_2 = 0, \quad (28)$$

resulting in amplitude values

$$A_1 = -A_2 = A/2. \quad (29)$$

and hence in the following wave dynamics:

$$U_1 = A \cdot \cos\left(\frac{k_1 - k_2}{2}x\right) \cos\left(\omega t - \frac{k_1 + k_2}{2}x\right) = A \cdot \cos(\alpha k_0 x) \cos(\omega t - k_0 x), \quad (30)$$

$$U_2 = A \cdot \sin\left(\frac{k_1 - k_2}{2}x\right) \sin\left(\omega t - \frac{k_1 + k_2}{2}x\right) = A \cdot \sin(\alpha k_0 x) \sin(\omega t - k_0 x). \quad (31)$$

This is a beating process corresponding to the periodic transfer of all wave energy from one waveguide line to the second line and back as shown in Fig. 4. Any coupling between identical waveguide lines leads to the very strong interaction responsible for such maximal swing of the energy circulation, but spatial period of the beats

$$\Lambda = 2\pi / (k_1 - k_2) \quad (32)$$

depends on the coupling factor value as follows:

$$\Lambda = 2\pi / (\alpha k_0). \quad (33)$$

This means that Λ is greater than the wave length by factor α^{-1} .

B. Nonidentical waveguide lines

To characterize interaction of two coupled waveguide lines quantitatively, in common with two coupled oscillatory circuits [13], one can introduce degree of coupling of two waveguide lines with different phase velocities v_{01} and v_{02} as follows:

$$\kappa = 2\sqrt{\alpha_1 \alpha_2} \frac{v_{01} v_{02}}{|v_{02}^2 - v_{01}^2|}. \quad (34)$$

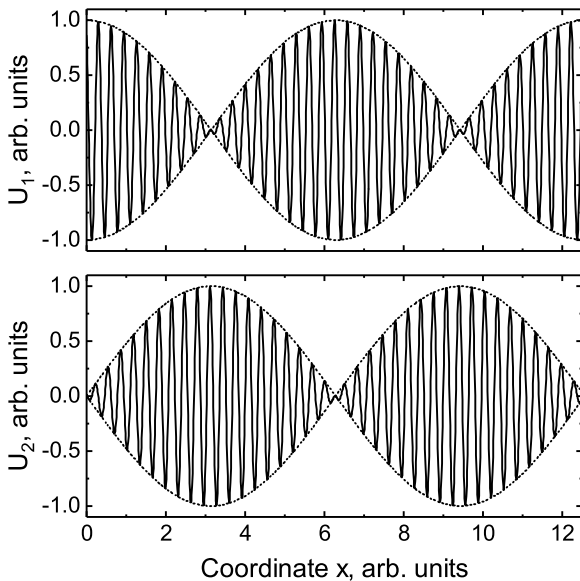


Fig. 4. The beating wave process in two coupled identical waveguide lines, when rf signal source $U = A \cos(\omega t)$ is connected to the input of the only first line.

The degree of coupling has always finite value for nonidentical lines, but tends to infinity for identical lines without reference to the coupling factor α of the lines.

In the case of nonidentical waveguide lines, the expressions for k^2 and v^2 have a much more complicated form as it follows from the master equation solution:

$$k^2 = \frac{\omega^2 (v_{02}^2 + v_{01}^2)}{2v_{01}^2 v_{02}^2} \pm \sqrt{\frac{\omega^4 (v_{02}^2 + v_{01}^2)^2}{4v_{01}^4 v_{02}^4} - \omega^4 \frac{1 - \alpha_1 \alpha_2}{v_{01}^2 v_{02}^2}}. \quad (35)$$

However, at weak interaction of the nonidentical lines, when

$$4\alpha_1 \alpha_2 \frac{v_{01}^2 v_{02}^2}{|v_{02}^2 - v_{01}^2|^2} \ll 1, \quad (36)$$

the intricate expression for k^2 can be simplified as follows (assuming that $v_{02}^2 > v_{01}^2$):

$$k_{1,2}^2 = \frac{\omega^2}{v_{01,02}^2} \pm \frac{\alpha_1 \alpha_2 \omega^2}{(v_{02}^2 - v_{01}^2)}, \quad (37)$$

and hence

$$k_1 = k_{01} + \Delta k_1, \quad k_2 = k_{02} - \Delta k_2, \quad (38)$$

$$v_1 = v_{01} - \Delta v_1, \quad v_2 = v_{01} + \Delta v_2, \quad (39)$$

where

$$k_{01} = \omega / v_{01}, \quad k_{02} = \omega / v_{02}, \quad (40)$$

$$\Delta k_1 \simeq \frac{\alpha_1 \alpha_2 v_{01}^2}{2(v_{02}^2 - v_{01}^2)} k_{01}, \quad \Delta k_2 \simeq \frac{\alpha_1 \alpha_2 v_{02}^2}{2(v_{02}^2 - v_{01}^2)} k_{02}, \quad (41)$$

and

$$\Delta v_1 = \frac{\alpha_1 \alpha_2 v_{01}^2}{2(v_{02}^2 - v_{01}^2)} v_{01}, \quad \Delta v_2 = \frac{\alpha_1 \alpha_2 v_{02}^2}{2(v_{02}^2 - v_{01}^2)} v_{02}. \quad (42)$$

Then, the equation set (18) and (19) gives the following amplitude ratios:

$$\chi_1 \equiv \frac{B}{A} \Big|_{k_1} = -\frac{\alpha_2 v_{01}^2}{(v_{02}^2 - v_{01}^2)}, \quad (43)$$

$$\chi_2 \equiv \frac{B}{A} \Big|_{k_2} = \frac{(v_{02}^2 - v_{01}^2)}{\alpha_2 v_{01}^2}. \quad (44)$$

In the case of low degree of coupling, coefficient $|\chi_1|$ is small, while $|\chi_2|$ is oppositely high.

When a rf signal source $U = A \cos(\omega t)$ is applied to the input of the only first line, boundary conditions

$$A_1 + A_2 = A, \quad \chi_1 A_1 + \chi_2 A_2 = 0, \quad \chi_1 A_1 + \chi_2 A_2 = 0 \quad (45)$$

yield in the following amplitude values:

$$A_1 = \frac{\chi_2}{(\chi_2 - \chi_1)} A, \quad A_2 = -\frac{\chi_1}{(\chi_2 - \chi_1)} A. \quad (46)$$

Thus, the wave process in the coupled nonidentical lines can be written as follows:

$$U_1 = A_1 \cos(\omega t - k_1 x) + A_2 \cos(\omega t - k_2 x) = D(x) \cos(\omega t - k_1 x + \theta(x)), \quad (47)$$

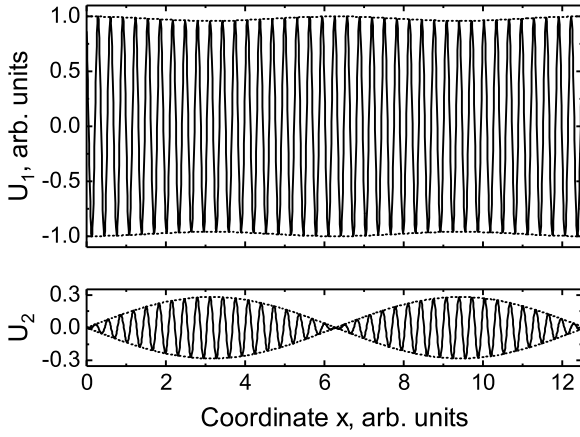


Fig. 5. The beating wave process in two coupled nonidentical waveguide lines at weak interaction of the lines ($\kappa \ll 1$), when rf signal source $U = A \cos(\omega t)$ is connected to input of the only first line.

$$U_2 = A_1 \cos(\omega t - k_1 x) - A_2 \cos(\omega t - k_2 x) = 2A \frac{|\chi_1| \chi_2}{(\chi_2 - \chi_1)} \sin\left(\frac{(k_1 - k_2)}{2} x\right) \times \sin\left(\omega t - \frac{(k_1 + k_2)}{2} x\right), \quad (48)$$

where

$$D(x) = A_1 \sqrt{1 + 2 \cos\left(\frac{(k_1 - k_2)}{2} x\right) \frac{A_2}{A_1} + \left(\frac{A_2}{A_1}\right)^2}, \quad (49)$$

$$\tan(\theta) = \frac{A_2 \sin\left(\frac{(k_1 - k_2)}{2} x\right)}{A_1 + A_2 \cos\left(\frac{(k_1 - k_2)}{2} x\right)} \approx \frac{A_2}{A_1} \sin\left(\frac{(k_1 - k_2)}{2} x\right). \quad (50)$$

This is also a beating wave process, but with much less energy, which is transferred from the first line to the second one and back, as shown in Fig. 5. Therefore, the wave propagating along the first line has the only minor cyclic variation in amplitude (49) and phase (50), while the wave penetrated into the second line represents low-amplitude beats accompanied with phase change by π every beat cycle. Increase in the coupling factors α_1, α_2 decreases the spatial beat period:

$$\Lambda = 2\pi / (k_1 - k_2) = 2\pi / [(k_{01} - k_{02}) + \Delta k_1 + \Delta k_2], \quad (51)$$

which is always less than $\Lambda_0 = 2\pi / (k_{01} - k_{02})$.

III. TWO-LINE JTWPA CRITICAL ISSUES

In the development of JTWPAs based on using two artificial waveguide lines, one must take into account several critical issues arising from both the line coupling and the line discreteness.

A. Influence of coupling

In the two-line JTWPA designs, the inevitable mutual electrical or magnetic coupling between the waveguide lines causes a background beat process, producing the cyclic transfer of the traveling waves energy from one line to another

and back. The nonlinear wave interaction required for the parametric amplifications has to coexist with this beat process.

In case of the flux-driven JTWPA mentioned above, the pump wave, propagating in the linear waveguide line, in reality will concurrently (i) modulate the inductances of the dc SQUID cells of the signal line and (ii) penetrate cyclically into this line with changing its phase by π every beat cycle. The spatial beat cycle length and the maximum amplitude of the penetrated wave depend on a geometric average of the coupling factors of the lines and degree of their coupling κ , respectively

As for the attractive idea to use the linear waveguide line as a pump energy source to balance (through the used coupling elements) depletion of the pump wave power in the other (signal) waveguide line and support the fixed pump wave amplitude in this line (when the pump and signal sources are connected separately to inputs of these linear and nonlinear waveguide lines, respectively), this cannot be properly realized since the only beating processes can occur in the two lines under mutual coupling. Besides, in force of the cyclic π -change in phase of the penetrated pump wave, the length of the amplifier line has to be restricted by the length Λ of the spatial beat cycle given by (33) and (51). Moreover, the limitation on the pump wave amplitude, imposed by the critical current value of the used Josephson junctions, can lead to an even stronger restriction on the amplifier length especially at high degree of coupling of the lines. These facts impose restrictions on the attainable gain of the JTWPA. In addition, one should take into account the inevitable beat-like leakage of both the signal and idler waves into the other line and cyclic variations in their phases that further decreases the gain.

The other significant drawbacks and restrictions follow from the inevitable phase mismatch between the pump wave and the signal and idler waves in the most interesting case of a low degree of coupling between the waveguide lines, when the only small part of the travelling wave energy is transferred cyclically between the lines. In the continuum approximation, the phase velocities (39) of the signal wave and the pumping wave, propagating in the first (nonlinear) line and in the second (linear) line respectively, are always different. In case of the flux driven JTWPA design, it makes impossible setting equal velocities of the of the signal wave and the inductance

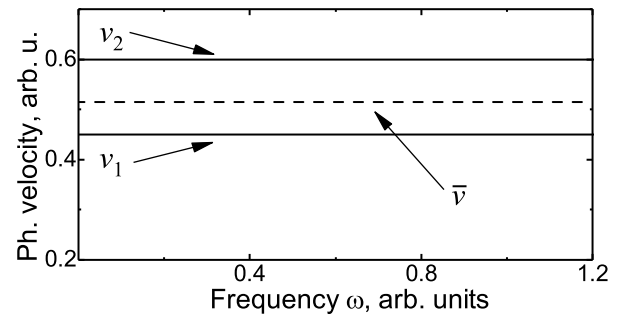


Fig. 6. Phase velocities v_1 and v_2 (solid lines) of the two eigen waves in the system of two coupled continuum waveguide lines at low degree of coupling. The dashed line shows the phase velocity \bar{v} corresponding to the mean wave vector $(k_1 + k_2) / 2$

modulation process caused by the pump wave. Moreover, the phase velocity \bar{v} of the pump wave penetrated into the signal line (see (48)) differs also from the signal velocity as shown in Fig. 6. However, these restrictions can be mitigated in the case of the discrete waveguide lines as shown below.

B. Influence of discreteness

An artificial lossless discrete LC waveguide lines (see Fig. 7) should be described by the following discrete telegraph equations:

$$I_n - I_{n+1} = i\omega C U_n, \quad (52)$$

$$U_n - U_{n+1} = i\omega L I_{n+1}, \quad (53)$$

where the propagating wave is considered as a harmonic wave. Let the cell size $a = x_{n+1} - x_n$ of the line be equal $a = 1$, then both the wave voltage and current can be written as follows [14]:

$$U_n = U_0 e^{i\omega t} e^{-ink}, \quad (54)$$

$$I_n = I_0 e^{i\omega t} e^{-ink}, \quad (55)$$

where U_0 and I_0 are the initial complex amplitudes of voltage and current, and k is the wave number. In this case, the discrete telegraph equations (52) and (53) result in the following dispersion expression:

$$\sin^2(k/2) = \frac{\omega^2}{\omega_{cut}^2} \quad (56)$$

and the phase velocity

$$v = \frac{\omega}{k} = \frac{\omega}{2 \arcsin(\omega/\omega_{cut})} = \frac{\omega}{2\theta}, \quad (57)$$

where ω_{cut} is the upper cut-off frequency of the discrete line:

$$\omega_{cut} = \frac{2}{\sqrt{LC}} \quad (58)$$

and

$$\theta = \arcsin\left(\frac{\omega}{\omega_{cut}}\right). \quad (59)$$

Moreover, such a discrete line generally has a complex wave impedance with the imaginary and real parts both depending on frequency [12]. In contrast to a continuous waveguide line, the wave impedance Z_0 of a discrete LC line composed of lumped L and C elements (as shown in Fig. 1) cannot be defined and measured as an exactly local ratio of the wave voltage to the wave current, since the voltage values are defined only at the line nodes, while the wave current values

are measured in the lumped L elements between the nodes. Therefore, the discrete telegraph equations (52) and (53) with (54) and (55) give the following wave impedance Z_0 (see also the other derivation of Z_0 as a repetitive impedance of the lumped cell array in [12]):

$$Z_0 = \sqrt{L/C} \cdot e^{\pm i\theta} = \pm i\omega L/2 + \sqrt{L/C - (\omega L)^2/4}, \quad (60)$$

where the two signs “+” and “-” correspond to the ratios V_n/I_n and V_n/I_{n+1} , respectively, and θ is defined by (59). This formula describes also the input impedance of the discrete line when it starts either with L element (sign “+”) or with initial C element (sign “-”). It can be seen that the imaginary part of Z_0 increases with frequency, while the real part of Z_0 decreases from the value $\sqrt{L/C}$ at low frequency down to zero at the cut-off frequency. When the discrete line is composed of symmetric T-cells “ $L/2-C-L/2$ ” and hence the line starts with initial $L/2$ element, its input impedance becomes completely real but again frequency-dependent:

$$Z_0 = \sqrt{L/C - (\omega L)^2/4}. \quad (61)$$

This dependence on frequency substantially obstructs perfect matching of the line in a wide frequency band. For example, when the discrete line is connected to the real-valued impedance $\rho = \sqrt{L/C}$, it results in the following imaginary and frequency-dependent reflection factor:

$$\Gamma = (\rho - Z_0) / (\rho + Z_0) = i \cdot \tan(\theta/2). \quad (62)$$

The existence of the upper cut-off frequency (58) makes possible keeping both the higher harmonics of the pump signal and the unwanted intermodulation components out of the frequency band. At the same time, the frequency-dependent phase velocity (57) in the frequency band does not allow achieving good phase matching between the pumping, signal and idler waves, needed to attain a good amplification. Therefore, an additional dispersion engineering techniques (e.g. see [8], [15]) has to be used to improve the wave phase-matching.

In a one-line JTWPA, the phase mismatching can be mitigated with using the 4-wave-mixing (4WM) mode (5) and (6). In the mode, all the frequencies ω_p , ω_s , ω_i are located near each other (contrary to 3WM mode) and hence can be set in the vicinity of $\omega_{cut}/3$, where the wave velocity slowly changes with frequency. Besides, both the harmonics of pump wave and the unwanted intermodulation components produced by the cubic nonlinearity appear above the cut-off frequency.

In the case of a hypothetical two-line JTWPA, one can recommend to use the 3-wave-mixing (3WM) mode (3) and (4) instead as a better mismatching trade-off. Fig. 8 shows the possible frequency scheme corresponding to 3WM mode, which can be realized in the flux-driven JTWPA. In the scheme, $\Delta\omega$ is the frequency range, where the phase velocities of the signal and idler waves in the Josephson (signal) line (curve v_1) are close to the phase velocity of the pump wave propagating in the linear line (curve v_2) and modulating inductances of the dc SQUID cells of the signal line. These velocities correspond to the eigen wave vectors k_1 and k_2 for the system of two coupled discrete waveguide lines with different cut-off frequencies at low degree of coupling of the lines. Of course, some small

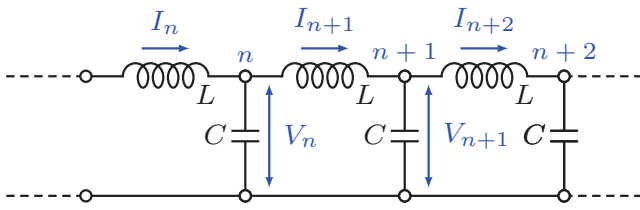


Fig. 7. An artificial discrete LC line.

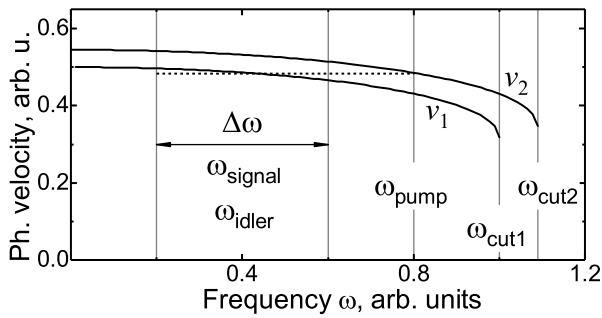


Fig. 8. The phase velocities v_1 and v_2 (corresponding to the eigen wave vectors k_1 and k_2 , respectively) of the waves propagating of the discrete coupled nonlinear (Josephson) and linear lines with different cut-off frequencies at low degree of coupling of the used lines, as well as the possible frequency scheme corresponding to 3WM mode, which can be realized in the flux-driven JTWPA. Here $\Delta\omega$ is the frequency range, where the phase velocities of the signal and idler waves in the Josephson line (lower curve) are close to the phase velocity of the pump wave propagating in the linear line (upper curve). The cut-off frequencies of the coupled nonlinear (Josephson) and linear lines are 1.0 au and 1.09 au, respectively.

part of the pump wave power will also penetrate into the signal line and decrease available linear dynamic range of the amplifier. As shown in [12], an additional increase in the reference dynamic range can be achieved with substituting dc SQUIDS for bi-SQUIDS.

If one considers the two-line design where the pumping wave in the nonlinear Josephson line is supplied through the used coupling elements by the high-power wave propagating in the other waveguide line which is linear, the 3WM mode can be suggested in accordance with the frequency diagram shown in Fig. 9. This diagram is similar to the one presented in Fig. 8, where the phase velocity of the pump wave v_2 in the linear line is replaced by the phase velocity \bar{v} (dashed line) corresponding to the mean wave vector $(k_1+k_2)/2$. This is the phase velocity of the pump wave penetrated into the nonlinear Josephson line as follows from (48). Unfortunately, a nontrivial trade-off has to be determined for both the parameters of the waveguide lines (resulting in the cut-off frequencies) and their mutual coupling in order to set the compromised values of (i) the phase velocity \bar{v} of the penetrated pump wave, (ii) the amplitude A_p of the wave (see (48)), and (iii) the spatial beat cycle length Λ given by expression (51).

IV. CONCLUSION

In summary, there are several critical obstacles to the two-line designs of Josephson traveling wave parametric amplifiers (JTWPA) such as the flux-driven JTWPA [11], [12] and the other ones, where an additional linear waveguide line is supposed to be used as a pump wave energy source for the nonlinear Josephson line in order to balance (through coupling elements) the pump wave power depletion and hence to support the fixed pump wave amplitude in this waveguide line. The obstacles result from both (i) the cyclic transfer of wave energy from one waveguide line to the other one and back and (ii) the phase mismatch between the pump, signal and idler waves following from the line coupling and the line discreteness. In particular, in the case of flux-driven

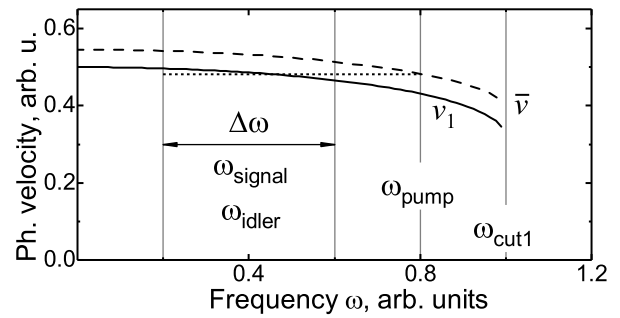


Fig. 9. The phase velocities v_1 (corresponding to the eigenwave vector k_1) of the wave propagating in the signal Josephson line (solid curve) and the phase velocity \bar{v} (corresponding to the wave vector $\bar{k} = (k_1 + k_2)/2$) of the pump wave penetrated into this signal line (dashed curve) at low degree of coupling of the used lines, as well as the possible frequency scheme corresponding to 3WM mode in the signal Josephson line. Here $\Delta\omega$ is the frequency range, where the phase velocities of the signal and idler waves are close to the phase velocity \bar{v} of the pump wave penetrated into the signal line. The cut-off frequencies of the coupled nonlinear (Josephson) and linear lines are 1.0 au and 1.2 au, respectively.

JTWPA, the required traveling-wave-patterned modulation of the SQUID-cell inductances of the Josephson signal line under the influence of a high-power pump wave, will be inevitably accompanied with an unwanted cyclic penetration of the pump wave to the nonlinear Josephson line. Besides, the cyclic phase variation and the cyclic power leakage of the signal and idler waves to the pump line will also interfere with the amplification process.

CONFLICT OF INTEREST STATEMENT

The authors declare no conflict of interest. The funder had no role in any part of the manuscript preparation process.

REFERENCES

- [1] C. Macklin, K. O'Brien, D. Hover, M. E. Schwartz, V. Bolkhovskiy, X. Zhang, W. D. Oliver, and I. Siddiqi, "A near-quantum-limited josephson traveling-wave parametric amplifier," *Science*, vol. 350, no. 6258, pp. 307–310, 2015.
- [2] M. Haider, J. Russer, J. Abundis Patino, C. Jirauschek, and P. Russer, "A josephson traveling wave parametric amplifier for quantum coherent signal processing," in *2019 IEEE MTT-S International Microwave Symposium (IMS)*. IEEE, 2019.
- [3] A. Fadavi Roudsari, D. Shiri, R. H. Nilsson, G. Tancredi, A. Osman, I. Svensson, M. Kudra, M. Rommel, J. Bylander, V. Shumeiko, and P. Delsing, "Three-wave mixing traveling-wave parametric amplifier with periodic variation of the circuit parameters," *Applied Physics Letters*, vol. 122, no. 5, 2023.
- [4] M. Esposito, A. Ranadive, L. Planat, and N. Roch, "Perspective on traveling wave microwave parametric amplifiers," *Applied Physics Letters*, vol. 119, no. 12, p. 120501, 2021.
- [5] T. Dixon, J. Dunstan, G. Long, J. Williams, P. Meeson, and C. Shelly, "Capturing complex behavior in josephson traveling-wave parametric amplifiers," *Physical Review Applied*, vol. 14, no. 3, p. 034058, 2020.
- [6] K. Peng, M. Naghiloo, J. Wang, G. Cunningham, Y. Ye, and K. O'Brien, "Floquet-mode traveling-wave parametric amplifiers," *PRX Quantum*, vol. 3, no. 2, p. 020306, 2022.
- [7] K. Peng, R. Poore, P. Krantz, D. Root, and K. O'Brien, "X-parameter based design and simulation of josephson traveling-wave parametric amplifiers for quantum computing applications," in *2022 IEEE International Conference on Quantum Computing and Engineering (QCE)*. IEEE, 2022.
- [8] A. Remm, S. Krinner, N. Lacroix, C. Hellings, F. Swiadek, G. Norris, C. Eichler, and A. Wallraff, "Intermodulation distortion in a josephson traveling-wave parametric amplifier," *Physical Review Applied*, vol. 20, no. 3, p. 034027, 2023.

- [9] A. Zorin, "Josephson traveling-wave parametric amplifier with three-wave mixing," *Physical Review Applied*, vol. 6, no. 3, p. 034006, 2016.
- [10] A. B. Zorin, M. Khabipov, J. Dietel, and R. Dolata, "Traveling-wave parametric amplifier based on three-wave mixing in a Josephson metamaterial," in *2017 16th International Superconductive Electronics Conference (ISEC)*. IEEE, 2017.
- [11] A. Zorin, "Flux-driven Josephson traveling-wave parametric amplifier," *Physical Review Applied*, vol. 12, no. 4, p. 044051, 2019.
- [12] A. Nikolaeva, V. Kornev, and N. Kolotinskiy, "Bi-SQUID versus dc SQUID in flux-driven traveling-wave parametric amplifier," *Applied Sciences*, vol. 13, no. 14, p. 8236, 2023.
- [13] V. Migulin, V. Medvedev, E. Mustel, and V. Paryguin, *Basic theory of oscillations*. Moscow: MIR, 1983.
- [14] E. Kogan, "On parametric amplification in discrete Josephson transmission line," *Physica C: Superconductivity and its Applications*, vol. 616, p. 1354402, 2024.
- [15] M. Perelshtein, K. Petrovnin, V. Vesterinen, S. Hamedani Raja, I. Lilja, M. Will, A. Savin, S. Simbierowicz, R. Jabdaraghi, J. Lehtinen, L. Grönberg, J. Hassel, M. Prunnila, J. Govenius, G. Paroanu, and P. Hakonen, "Broadband continuous-variable entanglement generation using a Kerr-free Josephson metamaterial," *Physical Review Applied*, vol. 18, no. 2, p. 024063, 2022.